Self-Heterodyning Optical Waveguide Beam Forming and Steering Network Integrated on Lithium Niobate Substrate

Kohji Horikawa, *Member, IEEE,* Yoshinori Nakasuga and Hiroyo Ogawa, *Member, IEEE*

Abstract—**A novel self-heterodyning optical waveguide beam forming and steering network (BFN) integrated on a Lithium Niobate (LN) substrate is introduced to realize optically controlled active phased array antennas. This integrated LN-BFN can simultaneously control eight array elements and is demonstrated for the first time. The key component in the self-heterodyning system, an optical frequency shifter (OFS), is composed of phase- and amplitude-balanced four parallel optical phase modulators. An optical signal processing circuit equipped with a weighted electrode structure simplifies the beam steering operation. A fully integrated LN-BFN connected by optical fibers can steer beam direction with the sensitivity of 1.5 degrees per volt.**

I. Introduction

Microwave signal processing in the optical domain has the possibility of achieving large and complex microwave circuits. Photonics-based phased array antennas have been investigated in recent years. Both coherent and noncoherent techniques are now being developed to realize optically controlled phased array antennas. [1] An achievable way is classified into two representative methods, a heterodyne method [2]–[5] and a true time delay method [6], [7]. Though the former is more technically complex than the latter, it can be expected to flexibly treat complex operations and to reduce size and weight because of its signal processing in the optical domain.

Lithium Niobate (LN) devices have been gaining popularity because of their various nonlinear characteristics. Mach-Zehnder intensity modulators using the electrooptic effect of LN devices are now available. The LN device can be modulated at the same high speed as semiconductor devices such as GaAs, InP. LN devices are inferior to Silica devices in the point of insertion loss but are definitely superior to semiconductor devices. Therefore, LN devices are best suited for small-scale integration including high speed signal processors.

This paper describes the configuration and performance of an optical beam forming and steering network integrated on an LN substrate (LN-BFN). First, the configuration is described.

Manuscript received January 16, 1995; revised April 21, 1995.
K. Horikawa and H. Ogawa are with NTT Wireless Systems Laboratories, Kanagawa-ken, 238-03 Japan.
Y. Nakasuga is with NTT Opto-electronics Laboratories, Ibaraki-ken, 319-11 Japan.
IEEE Log Number 9413681.

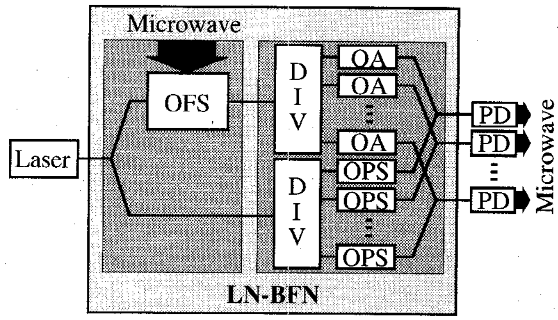

Fig. 1. Configuration of LN-BFN (Lithium Niobate Beam Forming Network). OFS: Optical Frequency Shifter. OA: Optical Attenuator. OPS: Optical Phase Shifter. DIV: Power Divider. PD: Photodetector.

Each component is then discussed in detail and experimentally verified. This paper demonstrates, for the first time, a fully integrated LN-BFN. This LN-BFN can steer beam direction by simply controlling the bias voltage.

II. System Configuration

The configuration of the proposed self-heterodyning optical beam forming and steering network integrated on a Lithium Niobate substrate (LN-BFN) is drawn in Fig. 1. The LN-BFN contains an optical frequency shifter (OFS), a lightwave modulator driven by microwaves, and an optical signal processing circuit (OSPC) that includes optical phase shifters and optical attenuators to control phase- and gain-feeding coefficients, respectively. An optical carrier is generated by a single optical source laser and its angular frequency is Ω. The optical carrier is divided into two and one is frequency-shifted to $(\Omega - \omega)$ by the microwave angular frequency of ω in the OFS. The frequency-shifted carrier is divided into N and the gain-feeding coefficients are controlled in the OSPC. In the same way, the passed-through carrier is divided into the same number and the phase-feeding ones are controlled in the OSPC. The gain-controlled carriers $Vg_n (n = 1\sim N)$ and phase-controlled carriers Vp_n are represented by

$$Vg_n = a_n \sin\{(\Omega - \omega)t\} \tag{1}$$

and

$$Vp_n = \sin(\Omega t + \phi_n). \tag{2}$$

All pairs of gain- and phase-controlled carriers are combined and taken to a photodetector (PD). The output microwave voltage Vm_n from the PD is obtained by heterodyne detection and is expressed by

$$Vm_n = \gamma a_n \cos(\omega t + \phi_n) \tag{3}$$

where γ is PD responsivity. In (3), a_n and ϕ_n are the gain- and phase-feeding coefficients controlled in the optical domain, respectively.

The prototype LN-BFN has eight array elements, namely N is eight. This number is the upper limit of circuit integration on a 3-inch size LN wafer. Details are described in the following sections.

III. Detailed Description

A. Optical Frequency Shifter (OFS)

1) Principle: The optical frequency shifter (OFS) has the structure of parallel Mach-Zehnder intensity modulators, namely, four optical phase modulators (OPM's) as shown in Fig. 2 [8]–[10]. At first, the behavior of one OPM is considered. When an optical carrier is phase-modulated by a single microwave tone, the equation for the voltage is

$$V = \nu \sin(\Omega t + \alpha\pi \sin(\omega t)) \tag{4}$$

where

ν = amplitude of the wave
Ω = angular frequency of the carrier
ω = angular frequency of the microwave
$\alpha\pi$ = modulation index

and α is modulation depth. This expression can be expanded in a spectrum consisting of a carrier and side frequencies in accord with

$$V = \nu \sum_{n=-\infty}^{\infty} J_n(\alpha\pi) \sin(\Omega t + n\omega t) \tag{5}$$

where $J_n(\alpha\pi)$ is a Bessel function of the first kind of order n and argument $\alpha\pi$. Equation (5) shows that the phase-modulated optical carrier has infinite order frequency elements, each of whose amplitude is given by the Bessel function which depends on the modulation index.

However, the OFS does not need all frequency elements, only the single-side first order frequency element. The OFS is composed of the four parallel OPM's as shown in Fig. 2 and relative phases of optical carriers into the four OPM's are tuned to 0, π, $\pi/2$ and $-\pi/2$. All amplitudes are made equal. In the same way, relative phases and amplitudes of microwave signals into the four OPM's are also tuned to 0, $\pi, \pi/2$ and $-\pi/2$ with uniform amplitude, respectively. Under this phase- and gain-balanced condition, the voltage at the combining point of the four OPM output-ports is given by

$$\begin{aligned} V &= \nu\cos(\Omega t + \alpha\pi\cos(\omega t)) - \nu\cos(\Omega t - \alpha\pi\cos(\omega t)) \\ &\quad + \nu\sin(\Omega t + \alpha\pi\sin(\omega t)) - \nu\sin(\Omega t - \alpha\pi\sin(\omega t)) \\ &= 4\nu \sum_{n=-\infty}^{\infty} J_{4n-1}(\alpha\pi)\sin\{\Omega t + (4n-1)\omega t\}. \end{aligned} \tag{6}$$

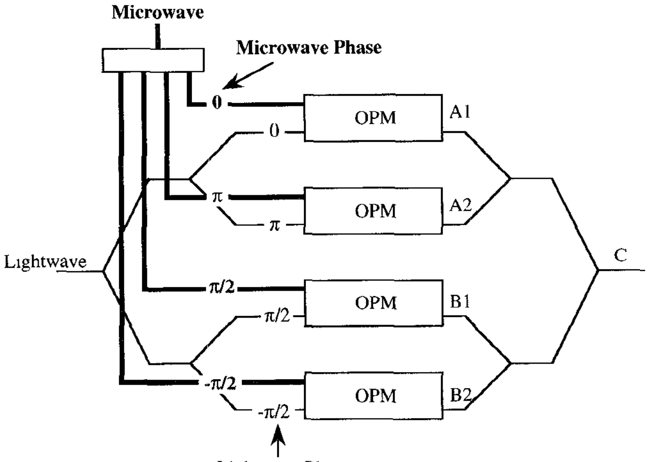

Fig. 2. Block diagram of OFS (Optical Frequency Shifter) composed of four balanced optical phase modulators. (OPM: Optcal Phase Modulator.)

Fig. 3 illustrates the relationship of (6) by using spectrum expressions. Almost all undesired frequency elements are canceled. The desired negative first order element and undesired positive third, negative fifth, etc. order elements are generated in the OFS.

When the microwave is regenerated by heterodyne detection of the OFS output and the fundamental element passed through another path, odd order undesired harmonics are also generated. The undesired harmonics level depends on the modulation index, but these do not affect the transmission frequency band.

If the above phase- and gain-relationship becomes slightly unbalanced, all kinds of orders, especially fundamental and undesired elements are created with low bit amplitude in the OFS. Each OPM has the output characteristics expressed by (5) and calculated amplitudes of each order element are shown in Fig. 4. When modulation depth α is about 0.8, the fundamental element that is undesired as the OFS output is not generated and the first order element that is indispensable almost becomes maximum. This result shows that best power efficiency under a stable condition can be achieved at this point even if the OFS has a slight imbalance.

2) Design: The wavelength of the optical carrier is 1.3 μm. A z-cut $LiNbO_3$ (LN) substrate was used with thickness of 300 μm. The waveguides were made by Ti diffusion and are single mode. This substrate has a 1.6-μm-thick SiO_2 buffer layer between the LN substrate and microwave electrodes to match a microwave velocity to a lightwave velocity. A thin Si film is used to disperse electric charge. The microwave electrodes are made of 15-μm-thick Au. Fig. 5 shows a pattern drawing of the OFS. Two parallel co-planar lines form the four phase modulator electrodes. The lightwave phase-balance among four OPM's is given by supplying optimum DC bias voltage to the $\pi/2$-shift electrode and microwave electrodes. On the other hand, microwave phase-balance is given by the phase of the external $\pi/2$-and-3-dB hybrid circuit and the co-planar lines. Y-branching power dividers and Y-fed power combiners divide and combine waveguides, respectively. Waveguide pitch between two output waveguides

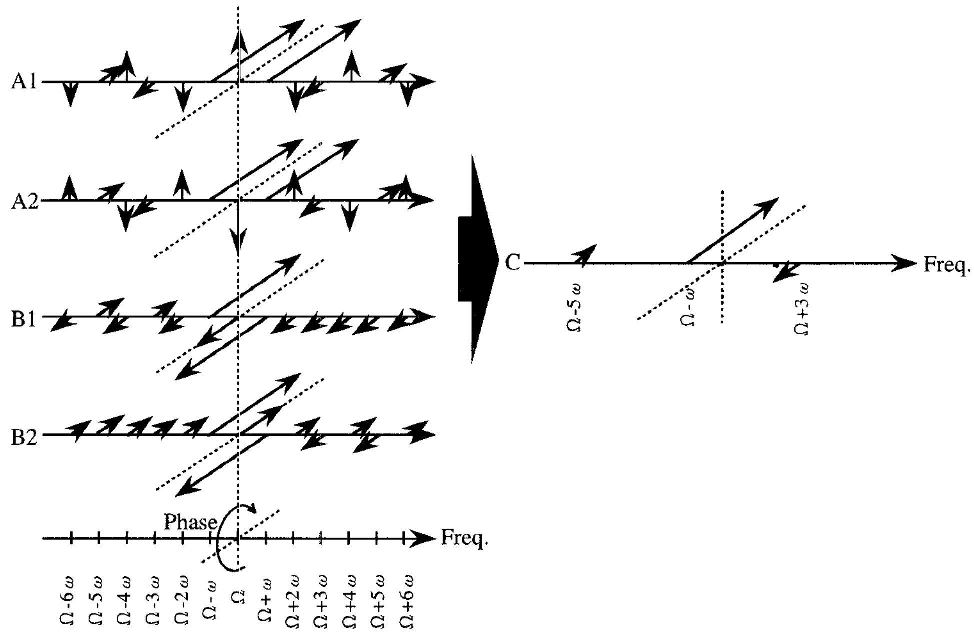

Fig. 3. OFS's operation principle drawn by spectrum expressions. According to four balanced phase relationship, OFS generates a desired negative first order element and undesired positive third, negative fifth, etc. order elements. A1, A2, B1, B2 and C are probed points shown in Fig. 2. Ω: Lightwave frequency. ω: Microwave frequency.

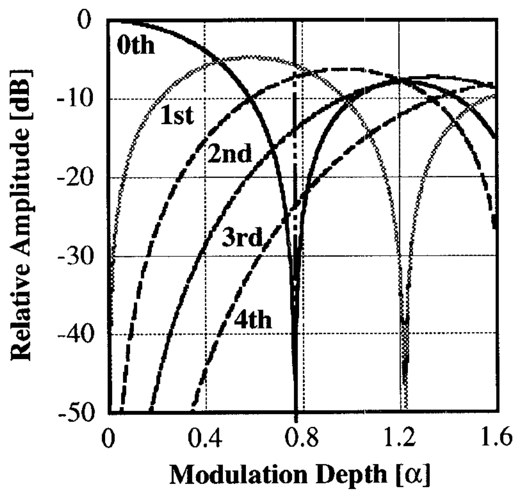

Fig. 4. Calculated amplitude curves of OPM output depending on modulation depth.

was designed to 250 μm to match the pitch of most array fibers on the market.

Characteristic impedance of these microwave lines needs to be 50 ohms to effectively couple microwaves to lightwaves. In addition, impedance mismatch has to be carefully avoided not only to decrease unnecessary microwave insertion loss but also to maintain characteristic balances among four OPM's. Parameters of these coplanar lines were estimated by using the extended spectral-domain method [11]. A designed 50-ohm coplanar line was measured and results are shown in Fig. 6. The parameters of this line are also shown in Fig. 6. These results almost coincided with the estimated value designed by the extended spectral-domain method.

This OFS operation was confirmed from 1 to 18 GHz by using a lightwave component analyzer, HP 8703A. These

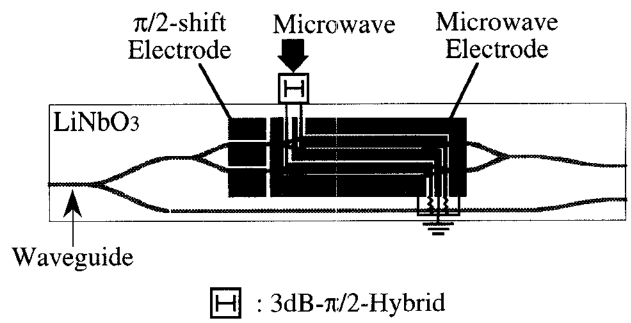

Fig. 5. Pattern drawing of OFS fabricated on $LiNbO_3$ substrate.

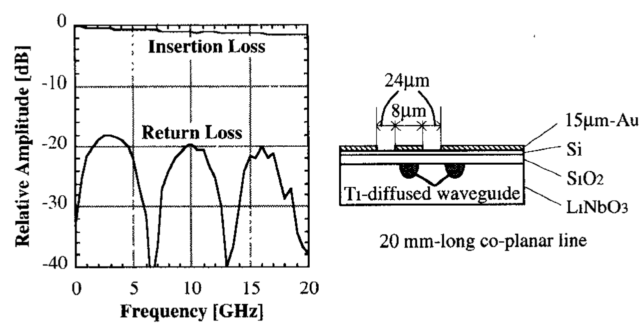

Fig. 6. Coplanar microwave electrode characteristics on the left-hand side and line parameters on the right-hand side.

frequencies were restricted by a used external microwave $\pi/2$-and-3-dB hybrid circuit.

3) Experimental Results: The characteristics of a microwave phase shifter (MPS) composed of an interferometer of an OFS and an optical phase shifter (OPS) were measured in order to evaluate OFS performance. The measured microwave frequency was restricted to 3 GHz by the PD used, an Ortel

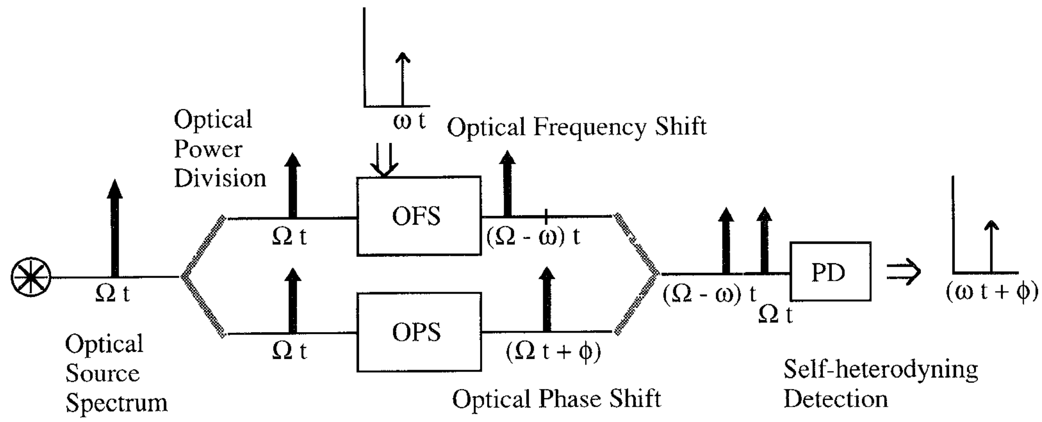

Fig. 7. Principle of self-heterodyning microwave phase shifter (MPS) composed of an interferometer of an optical frequency shifter (OFS) and an optical phase shifter (OPS). Ω: Lightwave angular frequency. ω: Microwave angular frequency.

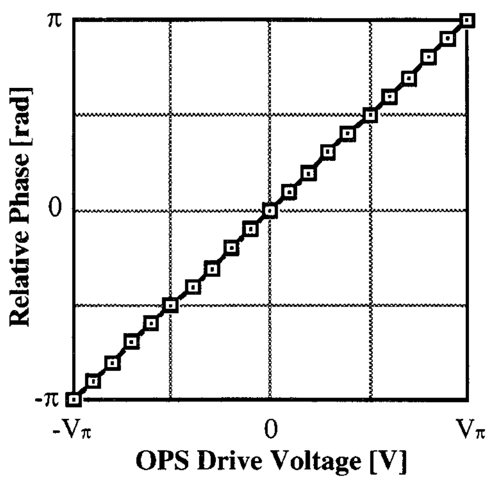

Fig. 8. MPS phase characteristics to OPS drive voltage from $-V\pi$ to $V\pi$.

2510A InGaAs photodiode. Chip size of the OFS is 67 by 2 mm.

Fig. 7 shows the principle of the MPS. The microwave is regenerated by the self-heterodyning between the frequency-shifted carrier and phase-shifted carrier. Since this OFS is a negative first order generator, the output microwave is unstable if undesired order elements, especially for fundamental and positive first order elements, are output from the OFS. The measured microwave phase characteristics of the MPS are shown in Fig. 8. The microwave phase was linearly changed by π radians against the OPS drive voltage of $V\pi$ (the half-wave voltage of the OPS) and then gain characteristics showed no fluctuation while the phase was being controlled. These results indicate that this OFS works as an almost ideal optical frequency shifter, and that the undesired frequency elements from the OFS are small enough.

B. Optical Signal Processing Circuit (OSPC)

1) Principle: As is well known, when linear antenna array elements are equally spaced, signal feeding with a uniform phase difference can form a beam. Beam steering can be achieved by changing the feeding phase difference value $[\Delta P]$. The beam direction $[D]$ is expressed by

$$D = \cos^{-1}\left(\frac{\Delta P}{kd}\right) - \theta_0 \tag{7}$$

where

$$k = \text{wave number } \left(\frac{2\pi}{\lambda}\right)$$
$$d = \text{spacing duration}$$

and θ_0 is reference angle. The θ_0 of $\pi/2$ means the vertical direction against the array axis.

In the z-cut LN waveguide, the transition of the refractive index Δn for polarized TM-wave is given by

$$\Delta n = \frac{1}{2} n_0^3 \gamma_{33} E_z \tag{8}$$

where

$$n_0 = \text{refractive index of waveguide}$$
$$\gamma_{33} = \text{Pockels constant}$$

and E_z is electric field amplitude on the z-axis. Lightwave phase delay $[P]$ produced by an optical phase shifter, which has the electrode length of $[L]$, is obtained by

$$P = \frac{2\pi}{\lambda_{\text{opt}}} \bullet \Delta n \bullet L \tag{9}$$

where λ_{opt} is the lightwave wavelength. The lightwave phase delay within the optical waveguides on the LN substrate is proportional to electric field strength and electrode length. Therefore, the structure of weighted electrode length on multiple optical phase shifters (OPS's) as shown in Fig. 9 enables the OPS's to simultaneously change their phases by supplying a common voltage. Thus, weighting the OPS electrodes, in terms of their length, simplifies the operation to achieve complex functionality.

2) Design: Parameters of the LN substrate used are the same as those of the OFS's. This optical signal processing circuit (OSPC) has many Y-branching power dividers and Y-fed power combiners. Each path from input to output goes through three Y-branching power dividers and one Y-fed

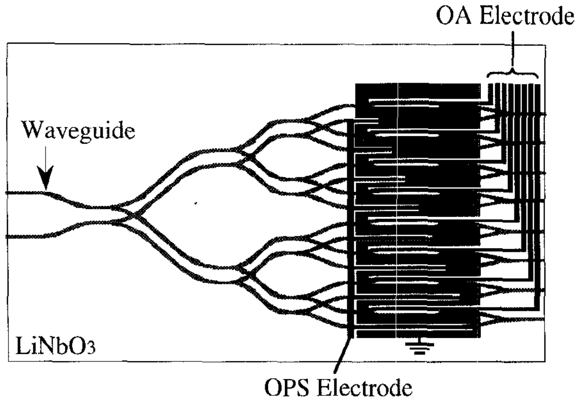

Fig. 9. Schematic drawing of an optical signal processing circuit (OSPC) fabricated on $LiNbO_3$ substrate.

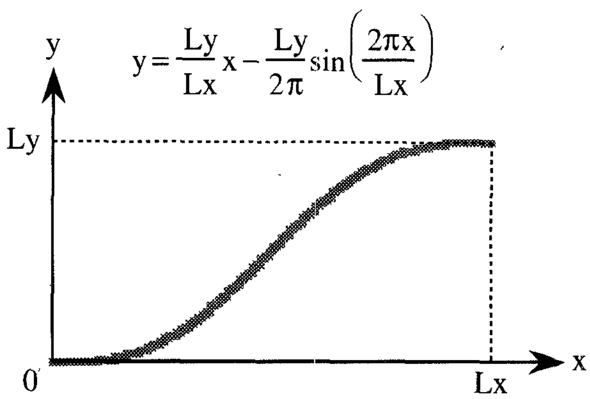

Fig. 10. Illustration of s-bend shape Lithium Niobate waveguide.

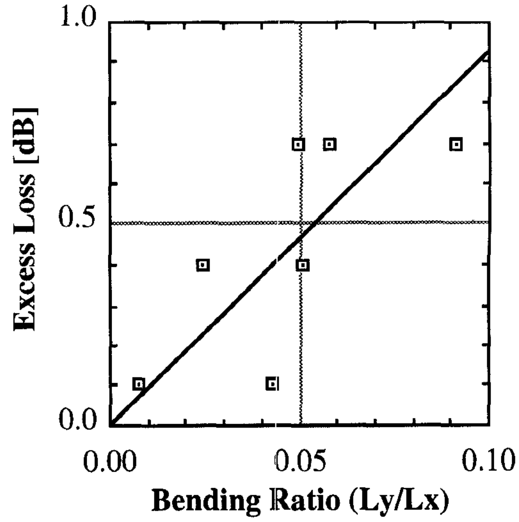

Fig. 11. Measured excess losses of s-bend shape LN waveguides. Open squares show measured points and a solid line shows curve-fitted characteristics.

power combiner, so the pure power dividing and combining loss L_{pure} amounts to 12 dB.

The waveguide pitch of input- and output-arrays has to be interfaced to 250 μm to match the pitch of the array fibers. In addition, intersections of waveguides cannot be avoided in achieving a 2-by-8 waveguide circuit on a planar substrate. It is known from experience that a cross angle of 5 $\sim$ 6 degrees at the intersecting point secures a cross-talk isolation of more than 20 dB. The insertion loss of the waveguide on the LN substrate is about 0.3 dB/cm for straight waveguides. As for s-bend waveguides, the insertion loss increases as the bend angle increases. S-bend shape of the LN waveguide is illustrated in Fig. 10. This shape is given by the following function:

$$y = \frac{Ly}{Lx}x - \frac{Ly}{2\pi}\sin\left(\frac{2\pi x}{Lx}\right) \tag{10}$$

where

$$Lx = \text{ length on } x\text{-axis}$$
$$Ly = \text{ length on } y\text{-axis.}$$

Fig. 11 shows the excess loss measured by using several s-bend waveguides that have different bending ratios of Ly/Lx. The excess loss L_{excess} characteristics estimated by the measured data as shown in Fig. 11 are expressed by

$$L_{\text{excess}} \approx 0.92\frac{Ly}{Lx} \text{ [dB].} \tag{11}$$

The OSPC shown in Fig. 9 has five s-bend waveguides in each path. The estimated total excess loss L_{bend} due to these s-bends is about 2 dB.

Total optical insertion loss L_{total} is obtained by using the transmission loss L_{trans}, which is dependent on length, and the waveguide-optical fiber contact loss L_{con}

$$L_{\text{total}} = L_{\text{pure}} + (L_{\text{trans}} + L_{\text{bend}} + L_{\text{con}}). \tag{12}$$

3) Experimental Results: Chip size of the OSPC is 68 by 3 mm. Polarization dependence has to be considered for the LN device. The TM-wave is effective in z-cut LN waveguides, so the lightwave from the laser is tuned to yield a vertical wave by a polarization controller and a polarizer. The wave is then fed to the waveguide through a polarization maintaining fiber (PMF).

The optical insertion loss of the OSPC was measured with input and output array fibers. The loss of each path was 17 $\pm$ 0.5 dB. All 2-point contact losses L_{con} were less than 2 dB as calculated from (12).

IV. Lithium-Niobate Beam Forming Network (LN-BFN)

A. Experimental Setup

The experimental setup for the LN-BFN is shown in Fig. 12. The optical source was a 30-mW Nd:YAG laser at 1.32 μm. The lightwave polarization was controlled to input a TM-wave into the LN-BFN. Both the OFS and the OSPC were assembled on an on-wafer measurement system. This on-wafer measurement system has 5-axis optical fiber positioners, coplanar microwave probers and DC probers. A two-PMF array connected the OFS to the OSPC. The vertical polarization from the OFS is maintained until the OSPC's input. An 8-core single-mode tape fiber was positioned at the 250 μm-pitch, eight output ports of the OSPC. At the opposite end of this tape fiber, an 8-module PD array, Ortel 2510A, regenerated microwave signals impressed with the feeding distribution. To

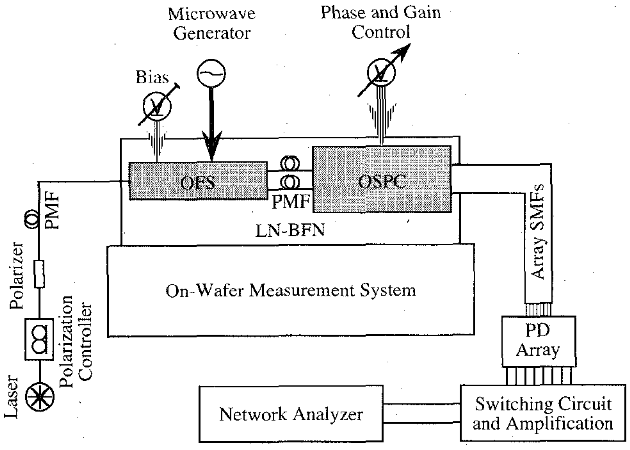

Fig. 12. Experimental setup for LN-BFN.

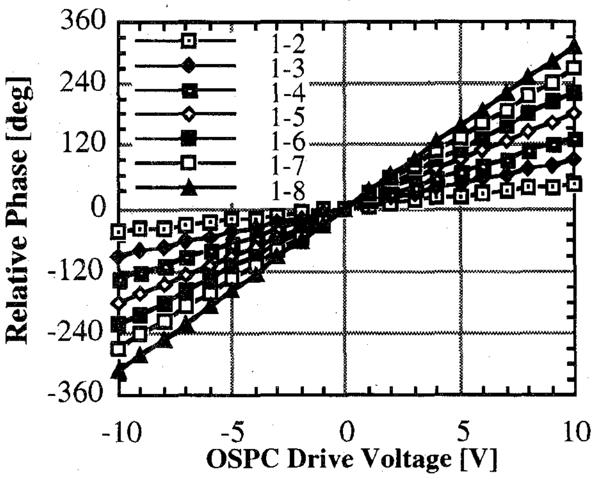

Fig. 13. Relative phase characteristics to phase control voltage applied to OSPC. These phases show phase feeding coefficients for 8-element phased array antenna.

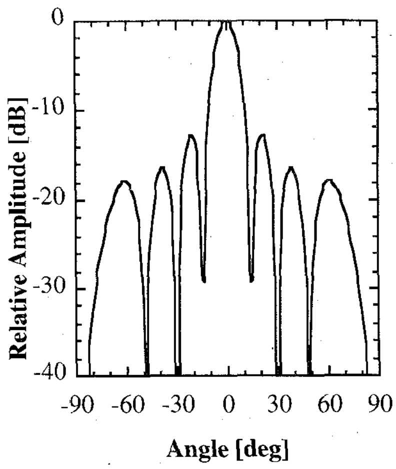

Fig. 14. Calculated array factor at phase difference of 0 degree.

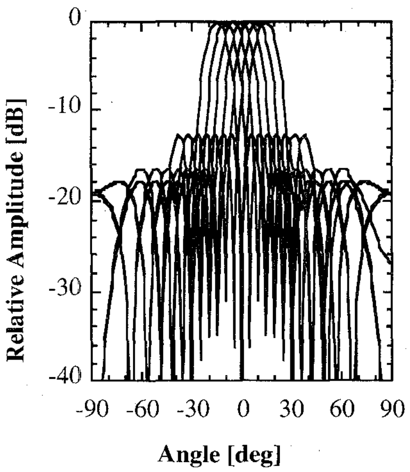

Fig. 15. Change in array factor with control voltage from −10 to 10 V.

measure phase and gain characteristics at a network analyzer, two signals were selected and amplified.

The frequency-shifted carrier power was −6 dBm at the OFS's output compared with the passed-through carrier power of 7 dBm when the applied microwave power was 20 dBm. The extinction ratio of the OFS, that is the ratio of optical power in unbiased condition to that at the optical phase-balanced condition described in Section III, reached 30 dB. Each PD module received optical power of about −10 dBm and regenerated microwave power of −40 dBm. The above results show that the LN-BFN offers sufficient performance for small-scale integration.

B. Performance

Seven relative phases between port-1 output and another output port were measured while changing the control voltage of the OSPC. Amplitudes of the eight signals were made uniform. Fig. 13 shows the relative phase characteristics to the phase control voltage applied to the OSPC. The test results were gained at the microwave frequency of 2.5 GHz. Indeed, almost the same OSPC characteristics were confirmed at other microwave frequencies, but its frequency is limited to 3 GHz due to PD frequency response. The phase characteristics drawn in Fig. 13 fall closely on straight lines. As the control voltage changes from −10 to 10 V, the phase difference between neighboring ports changes linearly from −45 to 45 degrees.

The calculated array factor at the phase difference of 0 degrees, that is the control voltage is 0 volts, is shown in Fig. 14. The calculation was conducted with

$$d = \frac{\lambda}{2}, \quad \theta_0 = \frac{\pi}{2}. \tag{13}$$

Since the uniform amplitude feeding distribution is given in this case, the sidelobe level of −13.2 dB appears. When lower sidelobe level is required, the LN-BFN can oblige by controlling the amplitude feeding distribution, as is well known, Cosine, Triangle, Taylor, Chebyshev, etc. Fig. 15 shows the array factors steered by the control voltages from −10 to 10 V. This LN-BFN can steer a beam with an angle of −15 to 15 degrees by the control voltage change of −10 to 10 V.

V. Conclusion

A self-heterodyning optical waveguide beam forming and steering network integrated on a Lithium Niobate substrate (LN-BFN) was reported and demonstrated. The feasibility of integrated optical BFN's was verified for the first time by the data gained from a prototype. The LN-BFN contains an optical frequency shifter (OFS) and an optical signal processing circuit (OSPC), and is totally functional circuit in conjunction with a lightwave source, a PD array, and connecting optical fibers. The OFS, a key component in self-heterodyning systems, is composed of an interferometer of four phase- and gain-balanced optical phase modulators. The OSPC is an interconnection circuit that includes waveguide intersections and has a weighted electrode length structure to simplify beam steering. Each component was described in detail and fully validated by experimental results.

The LN-BFN can control both phase- and amplitude-feeding distribution for eight array elements. The demonstrated LN-BFN can steer beam direction by simply controlling the OSPC at the sensitivity of 1.5 degrees per volt. The obtained signal level diagram showed that the LN-BFN is feasible for small-scale, 2-by-8, integration devices.

Acknowledgment

The authors would like to thank Dr. K. Kohiyama and Dr. S. Samejima for their continuous support and encouragement and Asst. Prof. T. Kitazawa for his instructive advice on LN circuit design. They also thank Ms. N. Sakamoto and Mr. F. Saito for assisting in the experiments.

References

[1] A. J. Seeds, "Evolution of optics in microwave radars," in *Proc. 24th Euro. Microwave Conf. Workshop*, Sept. 1994, pp. 58–67.
[2] J. F. Coward *et al.*, "A photonic integrated-optic RF phase shifter for phased array antenna beam-forming applications," *J. Lightwave Technol.*, vol. 11, no. 12, pp. 2201–2205, Dec. 1993.
[3] D. K. Paul, "Optical beam forming and steering for phased-array antenna," in *Proc. IEEE National Telesyst. Conf.*, June 1993, pp. 7–12.
[4] V. H. Hietala *et al.*, "High-performance GaAs/AlGaAs optical phase modulators for microwave photonic integrated circuits," *IEEE MTT-S Symp. Dig.*, May 1994, vol. 3, pp. 1497–1500.
[5] K. Horikawa *et al.*, "Self-heterodyning optical beam forming network for multibeam active phased array antenna," in *24th Euro. Microwave Conf. Proc.*, Sept. 1994, vol. 2 pp. 1673–1678.
[6] E. Ackerman *et al.*, "Integrated 6-bit photonic true time delay unit for lightweight 3–6 GHz radar beamformer," in *IEEE MTT-S Symp. Dig.*, 1992, vol. 2, pp. 681–684.
[7] C. T. Sullivan *et al.*, "Switched time delay elements based on AlGaAs/GaAs optical waveguide technology at 1.32 μm for optically controlled phased array antennas," *Proc. SPIE*, 1992, vol. 1703, pp. 264–271.
[8] M. Izutsu *et al.*, "Integrated optical SSB modulator/frequency shifter," *IEEE J. Quantum Electron.*, vol. QE-17, no. 11, pp. 2225–2227, Nov. 1981.
[9] R. A. Soref, "Voltage-controlled optical/RF phase shifters," *J. Lightwave Technol.*, vol. LT-3, pp. 992–998, Oct. 1985.
[10] G. A. Vawter *et al.*, "Photonic integrated circuit elements (PIC) for phased array steering systems," *Proc. SPIE*, vol. 1703, pp. 321–331, Apr. 1992.
[11] T. Kitazawa *et al.*, "Analysis of CPW for $LiNbO_3$ optical modulator by extended spectral-domain approach," *IEEE Microwave and Guided Wave Lett.*, vol. 2, no. 8, Aug. 1992.

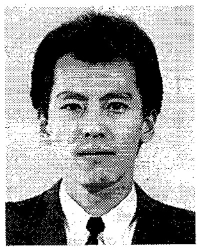

Kohji Horikawa (M'93) was born in Tochigi, Japan, in 1962. He received the B.S. degree in electrical engineering from Tokyo Institute of Technology, Japan, in 1984.

He joined Yokosuka Electrical Communication Laboratories, NTT, Yokosuka, in 1984. He has been engaged in research and development of satellite onboard transponder. Since 1993, he has been researching optical/microwave interaction systems and photonic beam forming network for microwave active phased array antennas.

Mr. Horikawa is a member of American Institute of Aeronautics and Astronautics, The International Society for Optical Engineering, and The Institute of Electronics, Information and Communication Engineers (IEICE) of Japan.

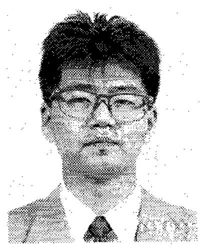

Yoshinori Nakasuga was born in Nagasaki, Japan, on April 8, 1966. He received the B.S. and M.S. degrees from Okayama University, Okayama, Japan, in 1989 and 1991, respectively.

In 1991, he joined the Radio Communication Systems Laboratories, NTT, Yokosuka, Kanagawa, where he was engaged in research on the optical beam forming network. At present, he is a Research Engineer at NTT Optoelectronics Laboratories, in Ibaraki, Japan, where he was engaged in research on the optical guided-wave devices.

Mr. Nakasuga is a member of the Institute of Electronics, Information, and Communications Engineers of Japan (IEICE).

Hiroyo Ogawa (M'84) received the B.S., M.S., and Dr. Eng. degrees in electrical engineering from Hokkaido University, Sapporo, in 1974, 1976, and 1983, respectively.

He joined the Yokosuka Electrical Communication Laboratories, Nippon Telegraph and Telephone Public Corporation, Yokosuka, in 1976. He has been engaging in the research on microwave and MMW integrated circuits, monolithic integrated circuits, the development of subscriber radio equipment, and the research on microwave and MMW photonics and fiber optic links for personal and satellite communication systems at NTT Wireless Systems Laboratories.

Dr. Ogawa is a member the Institute of Electronics, Information and Communication Engineers (IEICE) of Japan.